

# High resolution three dimensional morphometry and nasal air flow of the mammalian nose from multi-modal imaging

Thomas Neuberger<sup>1,2</sup>, Joseph P Richter<sup>3</sup>, Christopher R Rumpel<sup>3</sup>, Andrew P Quigley<sup>3</sup>, Allison N Ranslow<sup>3</sup>, Timothy M Ryan<sup>4</sup>, Timothy D Stecko<sup>4</sup>, Benison Pang<sup>5</sup>, Blaire Van Valkenburgh<sup>5</sup>, and Brent A Craven<sup>3</sup>

<sup>1</sup>Huck Institutes of the Life Sciences, Pennsylvania State University, University Park, PA, United States, <sup>2</sup>Department of Biomedical Engineering, Pennsylvania State University, University Park, PA, United States, <sup>3</sup>Applied Research Laboratory, Pennsylvania State University, University Park, PA, United States, <sup>4</sup>Center for Quantitative X-Ray Imaging, Pennsylvania State University, University Park, PA, United States, <sup>5</sup>Department of Ecology and Evolutionary Biology, University of California, Los Angeles, CA, United States

## Introduction:

The mammalian nasal cavity is a multi-purpose organ that houses a convoluted airway labyrinth responsible for respiratory air conditioning, filtering of environmental contaminants, and chemical sensing. The study of nasal form and function is of considerable importance in the fields of respiratory physiology<sup>1</sup>, otolaryngology<sup>2</sup>, inhalation toxicology<sup>3</sup>, and olfaction<sup>4</sup>. Because of the complexity of the nasal cavity, the anatomy and function of these upper airways remain poorly understood in most mammals. In this study, the nasal cavity of several mammals (dog, squirrel, coyote, bobcat, sea-otter, and deer) was investigated by magnetic resonance microscopy (MRM) and computed tomography (CT). For the MRI, a special procedure to image the air space inside the nose had to be developed. The reconstructed three-dimensional models are being used in computational fluid dynamics (CFD) simulations of nasal airflow, respiratory heat and moisture exchange, and odorant mass transport. To validate the computational models a transparent physical model of the squirrel has been constructed and state-of-the-art optical flow measurements will be conducted.

## Subjects & Methods:

All specimens were acquired in accordance with local laws and regulations. Following dissection, the nasal area of each specimen was immersed in 4% paraformaldehyde solution and stored for one week at 4° C to prevent degradation. In order to reduce MR scan time, the specimen were immersed for a second week in a phosphor buffered saline (PBS) solution containing up to 2% (depending on the specimen) Magnevist (Bayer, Germany). To allow for MR imaging of the air passages the specimen were kept in the Magnevist solution during imaging. To reduce the loading of the RF resonator and the field of view (FOV) during imaging the specimens were, after applying a vacuum to remove the majority of air bubbles inside the nose, transferred into party balloons removing excessive fluid from the outside of the specimen. While MRI was conducted on a 14.1 tesla vertical Agilent system (Agilent, Santa Clara, CA) using a 40 mm inner diameter millipede resonator in the case of the squirrel, all other specimens were imaged using a 7 tesla Agilent system and a 20cm ID quadrature driven birdcage resonator. High T2 contrast was introduced into the images by using a relatively long echo time in a slightly modified three dimensional spin echo sequence. Spatial resolutions between 40 μm isotropic in the case of the squirrel (experiment time 29h) and 100 μm isotropic in the case of the deer (experiment time 180h) were achieved. Due to the short T1 times short repetition times could be used (<150ms). During reconstruction (Matlab; The Mathworks, Inc., Natick, MA), zero filling by a factor of two in each direction resulted in an isotropic pixel resolution of up to 20 μm. Image processing of the MRI data and segmentation of the nasal airway was performed using AVIZO (VSG3D, USA). CT scans of the specimen were acquired on an OMNI-X HD-600 high resolution X-ray CT (HRCT) scanner (Varian Medical Systems, Lincolnshire, IL). After the fluid was blown out of the nasal pathways the heads were mounted in foam and positioned vertically in the CT scanner to collect coronal slices through the entire nasal region. Image processing of the CT data and reconstruction of the bony nasal structures was performed using AVIZO.

Computational fluid dynamics (CFD) simulations of nasal function and airflow were carried out using OpenFOAM (OpenCFD, Ltd.).

## Results:

Both MRI and CT images showed great details within the noses of the specimen. The maxilloturbinate region and the ethmoidal region of the squirrel are shown in Figure 1A (MRI) and 1B (CT) and in Figure 1C and 1D respectively. The red arrow in Figure 1B depicts the limitations of the CT imaging when nasal airways were blocked with water/mucus. Figure 1E - F shows the same areas within the deer nose. The red arrow in 1E identified an air bubble as a potential error source in the MR scanning. Given the three-dimensional segmentation of the nasal airway, various morphometry measures (airway perimeter, cross-sectional area, hydraulic diameter, surface area, internal volume, etc.) were calculated using a custom image processing program<sup>4</sup> (data not shown). Figure 2 shows the results of the CFD simulations in the dog and squirrel nose using the segmented three dimensional data. While the top image shows the pressure difference from the front to the back of the dog nose during sniffing, the middle and the bottom image show air pathways and velocity distributions of the air within the nose of the squirrel (middle) and the dog (bottom) during steady state flow.

## Discussion:

This study demonstrates the utility of combining MRI and CT data to obtain a complete description of the mammalian nasal cavity, namely the airway from MRI and the bony nasal structures from CT imaging. Magnetic resonance microscopy is superior at resolving the nasal airways and tissue, while CT is superior at resolving bony structures. Though many of the nasal passages can be delineated in the CT data, in some regions a distinction cannot be made between the tissue and any liquid that is inevitably present in the specimen. When combined, the three-dimensional reconstructions of the nasal airway and the bony nasal turbinates from MRI and CT, respectively, provide a complete description of the anatomical structure that was used in computational fluid dynamics simulations of nasal airflow. Further CFD simulations may include respiratory heat and moisture exchange and odorant mass transport.

## References:

[1] Lindemann, et al., *The Laryngoscope*, 114(6):1037–1041, 2009. [2] Rhee, et al., *Archives of facial plastic surgery*, 13(5):305–310, 2011. [3] Kimbell, et al., *Toxicological Sciences*, 64(1):100–110, 2001. [4] Craven et al., *The Anatomical Record*, 290(11): 1325-40; (2007).

## Acknowledgements:

Supported by NSF grants IOS-1120375 (to BAC and MHK), IOS-1118852 (to CJW), NSF IOB-0517748 (to BVV), and NSF IOS-1119768 (to BVV).

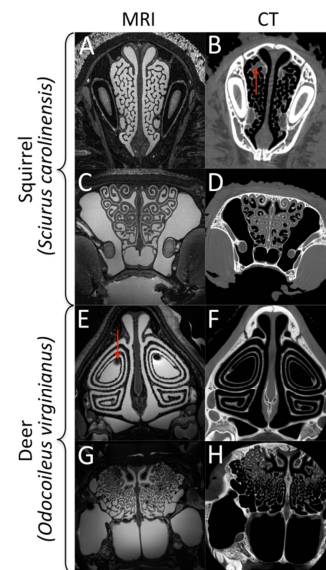


**Figure 1:** MRI (left) and CT (right) slices from the maxilloturbinate region and the ethmoidal region of the squirrel (A-D) and the deer (E-H). The red arrow in B indicates water/mucus blocking the nasal pathway in the CT scans and the one in E shows a trapped air bubble in the MRI scan.

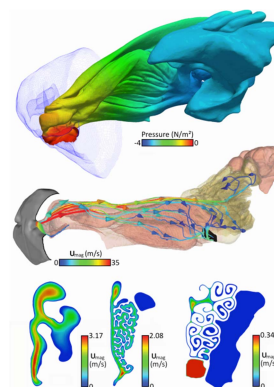


**Figure 2:** Results of the CFD simulations in the dog and squirrel nose. From top to bottom: Pressure difference within the dog nose during sniffing. Examples of air pathways within the squirrel nose. The color represents the air speed. Three cross sections showing the air velocity distribution in the front, middle and back region of the dog nose.